

https://doi.org/10.1070/QEL16640

Optimisation of a multi-disk cryogenic amplifier for a high-intensity, high-repetition-rate laser system

V.V. Petrov, G.V. Kuptsov, V.A. Petrov, A.V. Laptev, A.V. Kirpichnikov, E.V. Pestryakov

Abstract. **Holders of the active elements of a multi-disk multipass amplifier with a liquid-free closed cryogenic cooling cycle are modified. The equilibrium temperature of the active elements is experimentally investigated in relation to the power of diode pumping for the modified crystal holders. The dependence of the gain coefficient on the temperature of the active elements is measured. A small-signal gain of up to 1.2 is obtained in a single pass through the active element.**

Keywords: *diode pumping, high-peak-power laser system, high pulse-repetition rate, cryogenic temperatures, laser amplifier.*

1. Introduction

One of the promising lines of research in laser physics is the development, of the physical foundations, the means of implementation, and the architecture of pulsed radiation sources possessing simultaneously high peak and average powers [1–4]. These systems make it possible, in particular, to carry out research in the area of astrophysics by producing plasmas parametrically close to stellar plasmas [5]. Among other important applications of such systems is the acceleration of elementary particles when a high pulse-repetition rate of laser pulses provides the required particle flux in a short time interval [6]. The generation of attosecond radiation pulses for metrological investigations is also among the currently topical problems. Efficient generation of the high harmonics of optical frequencies requires ultimately short radiation pulses with carrier–envelope phase (CEP) stabilisation [7, 8], which simultaneously possess a high average power and a high peak one [9].

A source of attosecond radiation pulses with high peak and average powers is being developed at the Institute of Laser Physics, SB RAS. It is based on a short-period solid-state femtosecond laser system [10], which is employed as the source of radiation for subsequent parametric amplification, and a scalable all-solid-state diode-pumped laser system, which generates high-intensity high-repetition-rate radiation pulses [11, 12] for pumping a parametric amplifier. The short-period solid-state femtosecond laser system produces pulses at a repetition rate of 1 kHz, with the phase of the carrier frequency stabilised to 0.18 rad relative to the pulse envelope (CEP stabilisation).

2. Experimental setup

The scalable diode-pumped laser system schematised in Fig. 1 consists of a master oscillator, a preamplifier, and two synchronised parallel channels: a laser amplification channel of sub-Joule class and a parametric amplification channel [13].

A solid-state laser based on a liquid nitrogen-cooled diode-pumped $Yb^{3+}:Y_2O_3$ ceramics produces radiation pulses with an energy of ~1 nJ, duration of 1 ps, pulse repetition rate of ~80 MHz, centre wavelength of 1030 nm, and full spectrum width at half maximum of ~2 nm. The pulses are delivered to a fibre stretcher, which broadens their spectrum to 6 nm and increases their duration to ~0.5 ns. The pulse energy at the output of the stretcher amounts to ~0.15 nJ. Next, the pulses are fed to a diode-pumped Yb:KYW crystal regenerative amplifier. At the output the amplifier delivers 0.5-J pulses with a repetition rate of 1 kHz. Upon amplification, the radiation is split into two parts: one part, with a pulse energy of ~0.05 mJ (~10%), is delivered to the parametric amplification channel, while the other is the input radiation for the laser amplification channel. The splitting into the channels makes it possible to parametrically amplify both the radiation obtained by the superbroadening of the radiation of the master oscillator and the pulses of an external source, including CEP-stabilised ones.

The parametric amplification channel, which comprises a supercontinuum generation unit and an amplifier based on a nonlinear optical β-barium borate crystal, should provide a pulse energy of over 10 mJ at the channel output. To deliver a power of 1 TW at the output of the system, the supercontinuum production unit provides pulses with a spectral width of ~150 nm, which permits obtaining pulses shorter than 10 fs at the compressor output. The spectrum superbroadening is affected in a photon-crystal fibre with a high nonlinearity.

V.V. Petrov Institute of Laser Physics, Siberian Branch, Russian Academy of Sciences, prosp. Akad. Lavrent'eva 13/3, 630090 Novosibirsk, Russia; Novosibirsk National Research State University, ul. Pirogova 2, 630090 Novosibirsk, Russia; Novosibirsk State Technical University, prosp. K. Marksa 20, 630093 Novosibirsk, Russia; e-mail: vpetv@laser.nsc.ru;
G.V. Kuptsov, E.V. Pestryakov Institute of Laser Physics, Siberian Branch, Russian Academy of Sciences, prosp. Akad. Lavrent'eva 13/3, 630090 Novosibirsk, Russia; Novosibirsk National Research State University, ul. Pirogova 2, 630090 Novosibirsk, Russia;
V.A. Petrov Institute of Laser Physics, Siberian Branch, Russian Academy of Sciences, prosp. Akad. Lavrent'eva 13/3, 630090 Novosibirsk, Russia; Novosibirsk State Technical University, prosp. K. Marksa 20, 630093 Novosibirsk, Russia;
A.V. Laptev, A.V. Kirpichnikov Institute of Laser Physics, Siberian Branch, Russian Academy of Sciences, prosp. Akad. Lavrent'eva 13/3, 630090 Novosibirsk, Russia

Received 16 February 2018
Kvantovaya Elektronika **48** (4) 358–362 (2018)
Translated by E.N. Ragozin

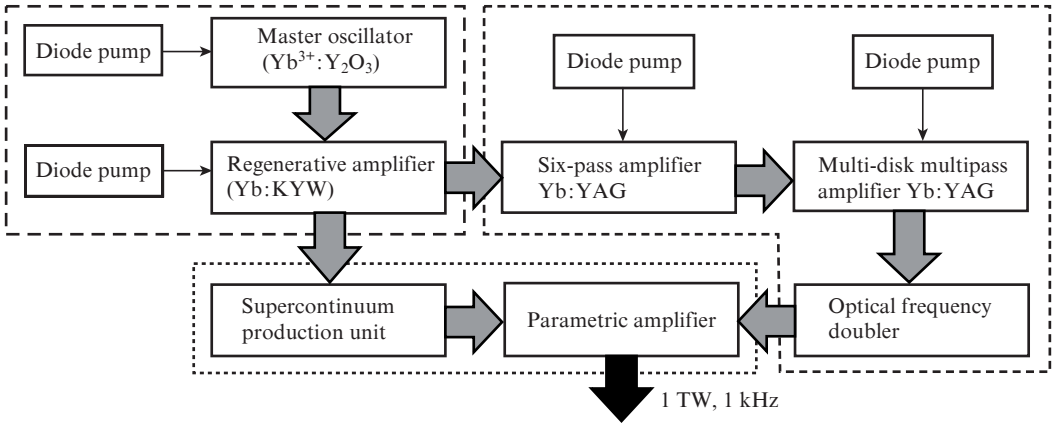

Figure 1. Schematic diagram of an all-solid-state diode-pumped scalable laser system, which generates radiation pulses at a high repetition rate.

The laser amplification channel consists of two diode-pumped laser amplification stages with a nonlinear optical crystal for optical frequency doubling. The first amplification stage comprises a cryogenic six-pass Yb:YAG (10 at. %) crystal laser amplifier pumped from both sides by diode-laser radiation with a total power of 250 W. At this stage, the pulses are amplified to an energy of 10 mJ. The second amplification stage is a multi-disk multipass amplifier with a liquid-free closed cryogenic cooling cycle (Fig. 2). It makes use of diffusion-bonded YAG–Yb:YAG (10 at. %) crystals pairwise attached to massive copper crystal holders [4].

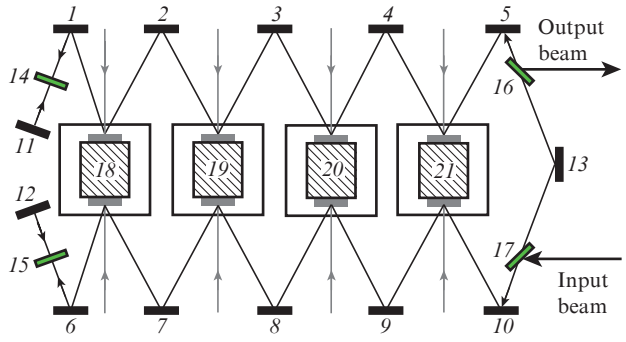

Figure 2. Schematic of the multipass amplifier with a liquid-free closed cryogenic cooling cycle:
(*1–13*) mirrors with high-reflectivity dielectric coatings; (*14*, *15*) quarter-wave plates; (*16*, *17*) polarisers; (*18–21*) copper crystal holders with two active elements. The grey arrows perpendicular to the cryostats show the diode pumping.

Every active element (AE) is pumped by diode laser pulses with an average output power of 100 W with a spectral width of 4 nm and a centre wavelength of 936 nm. In this case, the diameters of pump radiation beams for each pair of the AEs are equal to 4 and 7 mm, respectively. The AEs of the laser amplifier are cooled with pulse tube cryostats based on a closed helium circulation cycle. The coolers of this type permit reaching a temperature of 40 K and maintaining the working crystal temperature of ~120 K for a full diode pump power. The multipass amplifier was developed for producing pulses with an energy above 300 mJ for an input pulse energy of 10 mJ. At this stage of the work, our attention was focused on the generation of pulses with a repetition frequency of up to 1 kHz at the output of the laser amplification channel. However, to make the pulse amplification possible, it was necessary to modernise the cooling system of the multipass amplifier because of vibration of the compressors of the cooling system [14].

3. Cryogenic cooling system of the multi-disk multipass amplifier

The pulse tube coolers exhibit a low vibration level. However, at this testing stage of the multi-disk cryogenic amplifier we revealed short-term cyclic and long-term random angular shifts of the laser beam, which precluded the use of the output radiation of the laser amplification channel for pumping the parametric amplifier. Figure 3 depicts the characteristic coordinates of the centre of spatial radiation profile (of the beam centroid) recorded at 1-s intervals during 128 s.

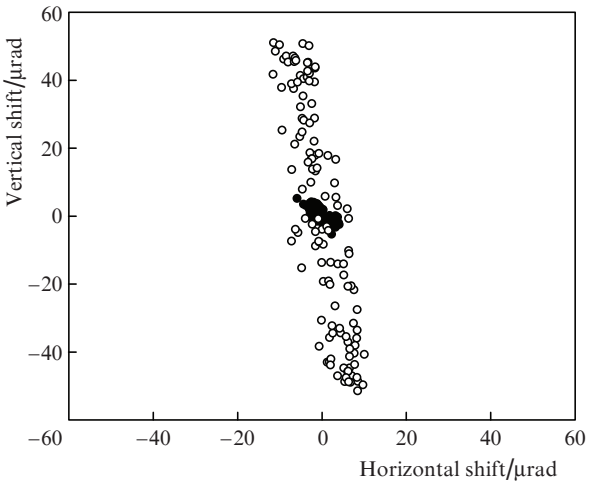

Figure 3. Map of centroid shifts of a probe laser beam upon reflection from an AE for a compressor switched (○) on and (●) off.

The short-term cyclic centroid shifts were represented by 50 ± 5 μrad beam deflections away from the propagation direction upon reflection from an AE with a frequency of several hertz, which coincided with the working frequency of the helium compression–expansion cycle of cryogenic coolers. The long-term shifts of the order of several milliradians

resulted in misalignment of the optical system during the period of full operation cycle (room temperature – cryogenic temperature – room temperature), which precluded from obtaining reproducible data. The data on the long-term shifts are depicted in Fig. 4. The long-term shifts are assumed to arise from the following two factors. First, when the compressor is turned on, there occurs a sharp pressure jump (~30 bar) in helium supply–evacuation lines, which exerts a mechanical effect on the vacuum chamber which accommodates the cryostat. Second, during the cooling–heating process there occurs a gradual change of the moments of tightening of threaded connections and a linear displacement of the parts of the crystal holder relative to each other because the cooling system comprises elements with different linear expansion coefficients.

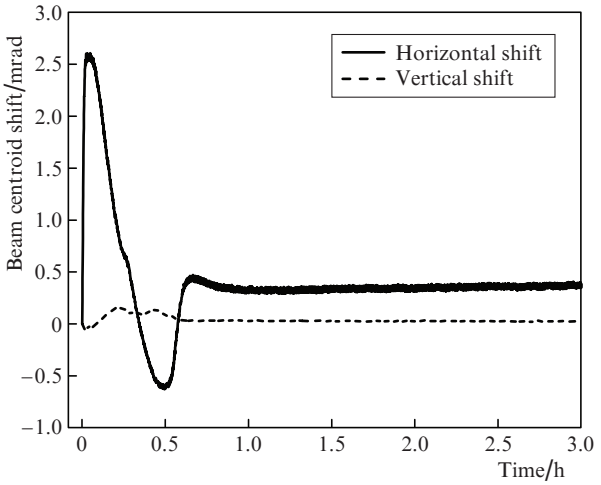

Figure 4. Long-term centroid shifts of a probe laser beam upon reflection from an AE during cooling. The onset of compressor operation corresponds to the zero on the time axis.

To solve the vibration problem of the cryogenic cooling systems, use was made of a flexible thermal bridge of the crystal holder. A disadvantage of this approach is a lowering of the cooling capacity due to an increase in the effective distance between the cryostat and the crystal holder, which results in an impairment of the laser characteristics of the AEs and the consequential lowering of the gain coefficient. To select the optimal thermophysical operation regime of the AE cooling system for the working parameters of the amplifier, one has to know the temperature distribution in the cooling system and in the AEs. To this end, we performed numerical simulations of the three-dimensional time-dependent heat conduction equation with the corresponding boundary conditions using the method of finite-difference approximation based on an implicit spatial splitting scheme. A spatially nonuniform mesh along the optical axis was implemented at the interface of materials with different physical parameters, making it possible to take into account, among other things, the thin multilayer contacts in the AE cooling system without a loss in simulation precision and computation speed [15]. To verify the results of simulations, an experimental investigation was made of the dependence of the AE temperature on the pump power with the use of the whole (initial) crystal holders. The investigation was carried out within the limits of the average pump power (70 W) of each laser diode source. The simulation data are in good agreement with the experimental ones [15].

The results of numerical simulations were employed to develop dissected crystal holders with a thermal bridge made up of 12 flexible heat conductors each of which is a stranded copper wire with a cross section of 10 mm^2. One part of a crystal holder is attached to a cryogenic cooling head and the other to the rigid base (Fig. 5). The use of dissected crystal holders permitted decreasing the beam centroid shifts upon reflection from the AE. The results of measurements of the short-term cyclic beam centroid shifts with the use of dissected and whole crystal holders are presented in Fig. 6. One can see that the behaviour of the laser beam at the amplifier output changed qualitatively after the modification of the AE cooling system. In the case of dissected crystal holders, the nature of oscillations is of the form of a normal distribution with an average value of 2.3 μrad and a variance of 1.2 μrad. The greatest deflection amounts to 5 ± 1.2 μrad. In the case of whole crystal holders, the distribution of the centroid shift histogram testifies to a pendulous nature of motion.

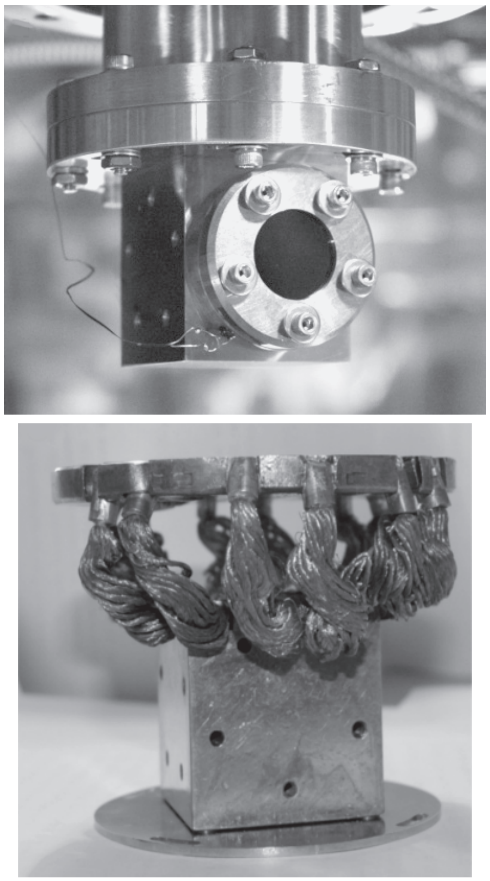

Figure 5. Photographs of (a) a whole crystal holder attached to a cooling head and (b) a dissected crystal holder with a flexible thermal bridge.

Figure 7 depicts the results of measurements of long-term random beam centroid shifts. They show a tendency for the return of the cooling system to the initial state after the primary shift. In this case, the use of dissected crystal holders made it possible to suppress the centroid shift down to ~0.2 mrad after turning on the compressor and thereby provide the reproducibility of results.

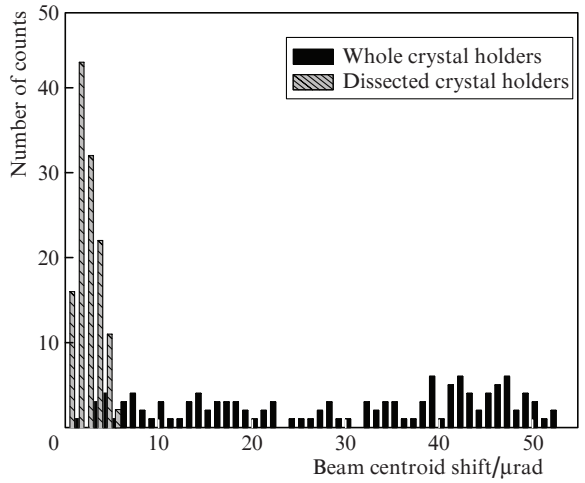

Figure 6. Statistics of short-term angular beam centroid shifts from the average position with the use of whole and dissected crystal holders.

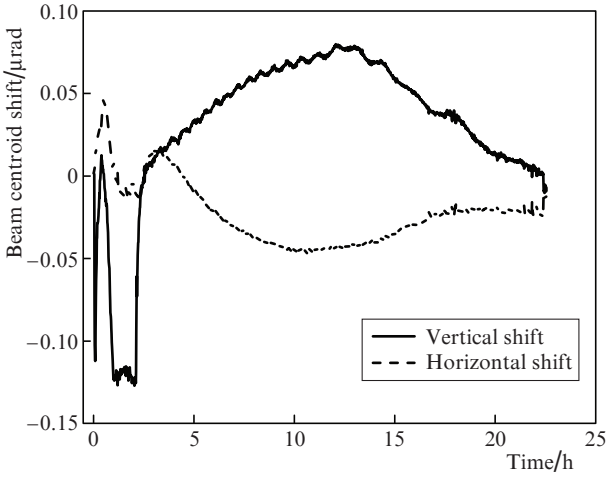

Figure 7. Long-term beam centroid shifts of a probe laser upon reflection from the AEs with the use of dissected crystal holders. The onset of compressor operation corresponds to the zero on the time axis.

We also carried out experiments to determine the thermophysical properties of the modified crystal holders. Two laser diodes were used to pump two AEs attached to a common crystal holder. The dependence of their equilibrium temperature on the average power of the diode pump with the use of the modified crystal holders is shown in Fig. 8. The experimentally determined average pump power that provided the operating thermal regime was found to be equal to 100 W. With the use of the whole crystal holder structure, the operating thermal regime was maintained for a pump power of 200 W. We believe that the insufficient efficiency of the dissected crystal holders is due to the features of their fabrication technology.

4. Signal amplification

The remodelling of the AE cooling system made it possible to lower the amplitude of cyclic short-term beam shifts to a level of less than 5 μrad. After the remodelling, we performed experimental measurements of the single-pass radiation gain of the AE. The experimental setup is shown in Fig. 9. The

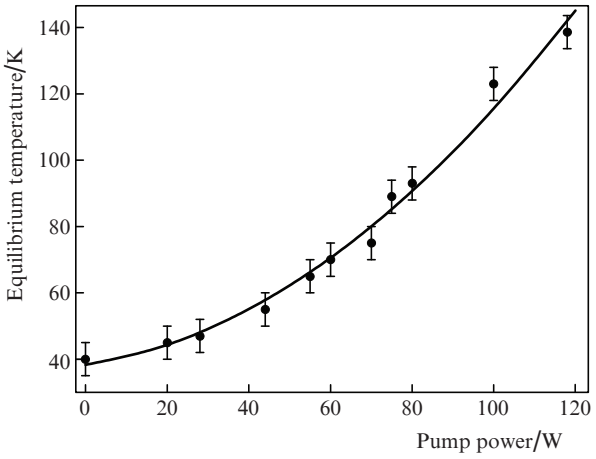

Figure 8. Equilibrium AE temperature as a function of the average pump power P: points – experimental data, solid curve – parabolic approximation $T = a + bP + cP^2$ ($a = 38.3$, $b = 0.18$, $c = 5.88 \times 10^{-3}$).

input pulse energy was measured at point I. Then, the radiation was directed to the AE (the first pass) using a set of mirrors. The pulse energy after the first pass was measured at point II. Next, the radiation was transmitted to a mirror through a $\lambda/4$ plate and reflected back to pass through the AE for the second time. The pulse energy after the second pass was measured at point III. The experiments were performed for a diode pump beam 4 mm in diameter, and average power of 100 W, a duty cycle of 0.5, and a pulse repetition rate of 1 kHz. Input pulses had the following parameters: an energy of 300 μJ, a duration of 500 ps, a beam diameter of 4 mm, and a pulse repetition rate of 1 kHz. Figure 10 shows the spatial intensity distribution of the pump radiation, the input radiation at point I, and the radiation after amplification (at point III). The time it takes the cooling system to reach the temperature regime amounts to several tens of minutes, making it possible to perform experiments at different AE temperatures. Figure 11 depicts the measured single-pass radiation gains for the AE. The resultant small-signal single-pass gain amounts to 1.1–1.2 at a temperature of 111 K, which is consistent with theoretical data [16] and permits obtaining 300 mJ

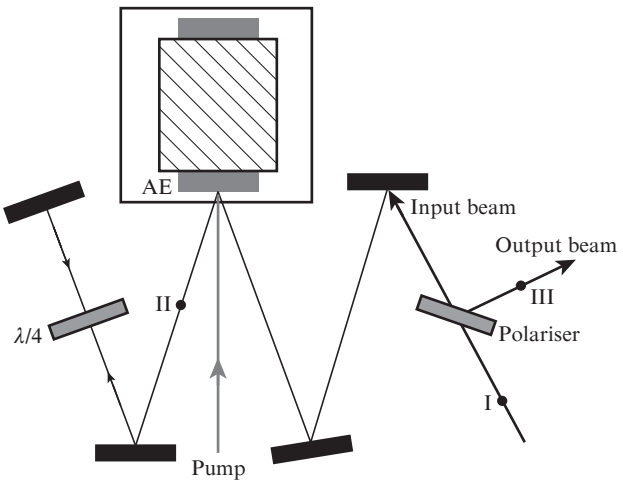

Figure 9. Schematic of the experiment to determine the single-pass radiation gain of the AE.

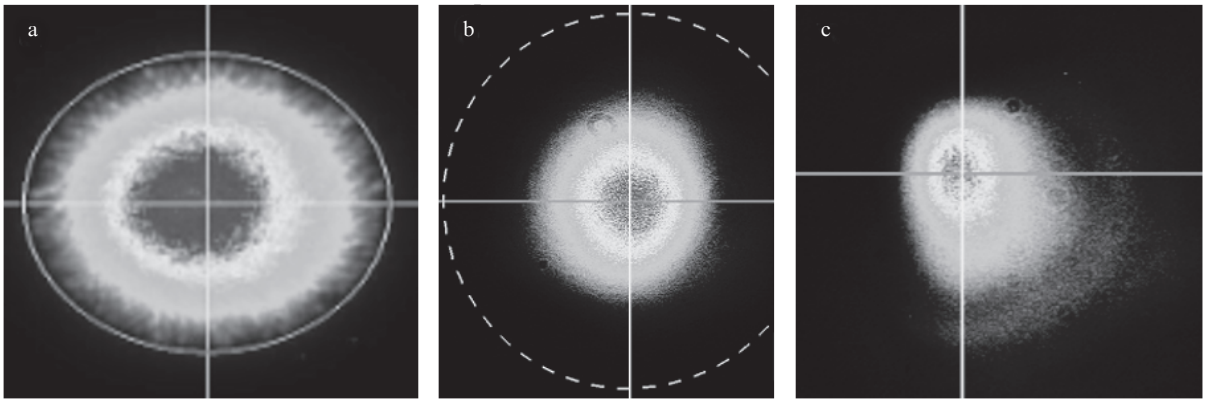

Figure 10. Spatial intensity distribution of (a) diode pump radiation, as well as of (b) input and (c) amplified radiation.

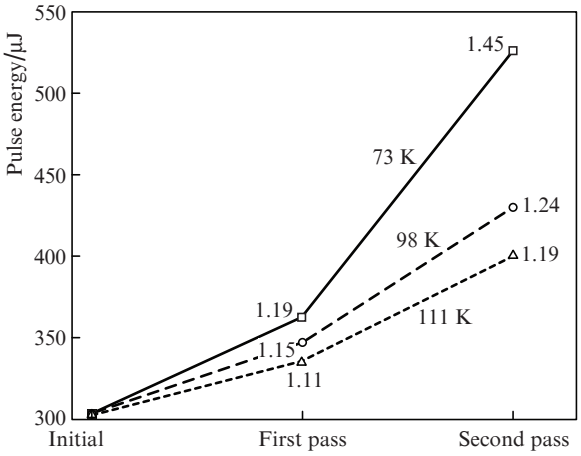

Figure 11. Dependences of the pulse energy on the number of their passes through the AE for different AE temperatures. The figure by the symbols stand for single-pass gains.

pulses at the output of the multi-disk multipass amplifier of the scalable laser system.

5. Conclusions

In this work we optimised a multi-disk multipass amplifier with a liquid-free closed cryogenic cooling cycle. The dependences of the equilibrium AE temperature on the diode pump power for modified crystal holders of the cooling system of the multipass amplifier were experimentally investigated. We determined the acceptable average diode pump power, which does not lead to an excess of the AE temperature over the working range. A single-pass signal gain of 1.1–1.2 was obtained for the AE. These results will be used in the development and construction of a scalable all-solid-state diode-pumped laser system producing high-intensity laser pulses with a high repetition rate.

Acknowledgements. This work was supported by the Presidium of the Russian Academy of Sciences (Programme 'Extreme Light Fields and Their Interaction with Matter') and the Siberian Branch of the RAS.

References

1. Puppin M., Deng Y., Prochnow O., Ahrens J., Binhammer T., Morgner U., Krenz M., Wolf M., Ernstorfer R. *Opt. Express*, **23** (2), 1491 (2015).
2. Baumgarten C., Pedicone M., Bravo H., Wang H., Yin L., Menoni C.S., Rocca J.J., Reagan B.A. *Opt. Lett*., **41** (14), 3339 (2016).
3. Zapata L.E., Reichert F., Hemmer M., Kartner F.X. *Opt. Lett*., **41** (3), 492 (2016).
4. Brown D.C., Tornegard S., Kolis J. *High Power Laser Sci. Eng*., **4**, e15 (2016).
5. Remington B.A., Drake R.P., Takabe H., Arnett D. *Phys. Plasmas*, **7** (5), 1641 (2000).
6. Borghesi M., Fuchs J., Bulanov S.V., MacKinnon A.J., Patel P.K., Roth M. *Fusion Sci. Technol*., **49** (4), 412 (2006).
7. Kirpichnikov A.V., Petrov V.V., Kuptsov G.V., Laptev A.V., Petrov V.A., Pestryakov E.V., Trunov V.I. *Zh. Prikl. Spektrosk.*, **83** (6-16), 668 (2016).
8. Drescher M., Hentschel M., Kienberger R., Tempea G., Spielmann C., Reider G.A., Corkum P.B., Krausz F. *Science*, **291** (5510), 1923 (2001).
9. Wu Y., Cunningham E., Zang H., Li J., Chini M., Wang X., Wang Y., Zhao K., Chang Z. *Appl. Phys. Lett*., **102**, 201104 (2013).
10. Kirpichnikov A.V., Petrov V.V., Kuptsov G.V., Laptev A.V., Petrov V.A., Pestryakov E.V., Trunov V.I. *Proc. SPIE* (2018) (in press).
11. Petrov V.V., Pestryakov E.V., Laptev A.V., Petrov V.A., Kuptsov G.V., Trunov V.I., Frolov S.A. *Quantum Electron*., **44** (5), 452 (2014) [*Kvantovaya Elektron*., **44** (5), 452 (2014)].
12. Kuptsov G.V., Petrov V.V., Laptev A.V., Petrov V.A., Pestryakov E.V. *Quantum Electron*., **46** (9), 801 (2016) [*Kvantovaya Elektron*., **46** (9), 801 (2016)].
13. Kuptsov G.V., Petrov V.V., Petrov V.A., Kirpichnikov A.V., Laptev A.V., Pestryakov E.V. *Zh. Prikl. Spektrosk.*, **83** (6-16), 533 (2016).
14. Petrov V.V., Laptev A.V., Kuptsov G.V., Petrov V.A., Kirpichnikov A.V., Pestryakov E.V. *Proc. SPIE* (2018) (in press).
15. Petrov V.A., Kuptsov G.V., Petrov V.V., Kirpichnikov A.V., Laptev A.V., Pestryakov E.V. *AIP Conf. Proc*., **1893**, 030121 (2017).
16. Petrov V.V., Pestryakov E.V., Petrov V.A., Kuptsov G.V., Laptev A.V. *Laser Phys*., **24** (7), 074014 (2014).